DMD Fast Forward. Published on June 8, 2018 as DOI: 10.1124/dmd.118.080861
This article has not been copyedited and formatted. The final version may differ from this version.

DMD # 80861

Consequences of Phenytoin Exposure on Hepatic Cytochrome P450 Expression during Postnatal Liver Maturation in Mice

Stephanie C. Piekos, Liming Chen, Pengcheng Wang, Jian Shi, Sharon Yaqoob, Hao-Jie Zhu, Xiaochao Ma, and Xiao-bo Zhong

Department of Pharmaceutical Sciences, School of Pharmacy, University of Connecticut, Storrs, Connecticut (S.C.P., L.C., S.Y., X.B.Z.); Department of Pharmaceutical Sciences, School of Pharmacy, University of Pittsburgh, Pittsburgh, Pennsylvania (P.W., X.M.); Department of Clinical Pharmacy, College of Pharmacy, University of Michigan, Ann Arbor, Michigan (J.S., H.J.Z.)

DMD Fast Forward. Published on June 8, 2018 as DOI: 10.1124/dmd.118.080861
This article has not been copyedited and formatted. The final version may differ from this version.

Running Title: Induction of CYPs by phenytoin in developmental liver

Corresponding author: Dr. Xiao-bo Zhong, Department of Pharmaceutical Sciences, School of Pharmacy, University of Connecticut, 69 N Eagleville Road, Storrs, Connecticut 06269, USA. Telephone: 860-486-3697; Fax: 860-486-5792; E-mail: xiaobo.zhong@uconn.edu.

Number of text pages: 34

Number of figures: 4

Number of tables: 0

Number of references: 51

Number of words in Abstract: 245

Number of words in Introduction: 752

Number of words in Discussion: 1496

ABBREVIATIONS: ADR: adverse drug reaction; AED: antiepileptic drug; BSA: bovine serum albumin; CAR: constitutive androstane receptor; DDI: drug-drug interaction; CYP: cytochrome P450; DTT: dithiothreitol; IAA: Iodoacetamide; PBS: phosphate-buffer saline; PXR: pregnane X receptor. SWATH-MS: sequential window acquisition of all theoretical mass spectra; TFA: trifluoroacetic acid.

ABSTRACT

The induction of cytochrome P450 enzymes (CYPs) in response to drug treatment is a significant contributing factor to drug-drug interactions, which may reduce therapeutic efficacy and/or cause toxicity. As most studies on CYP induction are performed in adults, enzyme induction at neonatal, infant, and adolescent ages is not well understood. Previous work defined the postnatal ontogeny of drug-metabolizing CYPs in human and mouse livers; however, there are limited data on the ontogeny of the induction potential of each enzyme in response to drug treatment. Induction of CYPs at the neonatal age may also cause permanent alterations in CYP expression in adults. The goal of this study was to investigate the short-/long-term effects of phenytoin treatment on mRNA and protein expressions and enzyme activities of CYP2B10, 2C29, 3A11, and 3A16 at different ages during postnatal liver maturation in mice. Induction of mRNA immediately following phenytoin treatment appeared to depend on basal expression of the enzyme at a specific age. While neonatal mice showed the greatest fold-changes in CYP2B10, 2C29, and 3A11 mRNA expression following treatment, the levels of induced protein expression and enzymatic activity were much lower than that of induced levels in adults. The expression of fetal CYP3A16 was repressed by phenytoin treatment. Neonatal treatment with phenytoin did not permanently induce enzyme expression in adulthood. Taken together, our data suggest that inducibility of drug metabolizing CYPs is much lower in neonatal mice than it is in adults and neonatal induction by phenytoin is not permanent.

DMD Fast Forward. Published on June 8, 2018 as DOI: 10.1124/dmd.118.080861
This article has not been copyedited and formatted. The final version may differ from this version.

Introduction

Drug-drug interactions (DDIs) are a major cause of adverse drug reactions (ADRs) and occur when one medication interferes with the efficacy or toxicity profile of another medication administered concurrently. Pharmacokinetic DDIs occur when the perpetrating drug affects the absorption, distribution, metabolism, or excretion of other 'victim' drugs, shifting plasma concentrations outside of optimal therapeutic windows (Palleria, Di Paolo et al. 2013). Plasma concentrations are largely determined by cytochrome P450 (CYP)-mediated drug metabolism, which can be inhibited or induced by xenobiotics. Several marketed drugs induce the transcription of CYP genes via the activation of nuclear receptors and are implicated in clinically significant DDIs (Lin 2006). Patients may experience attenuated therapeutic efficacy if induced CYP-mediated metabolism decreases plasma concentration of other active drug compounds taken simultaneously. Conversely, patients could experience adverse effects due to accumulation of toxic metabolites (Zanger and Schwab 2013).

Like adults, many infants and children are exposed to multiple medications at once, especially those that are hospitalized (Dai, Feinstein et al. 2016). However, DDIs in the context of pediatric patients are not as well understood as DDIs. This is mainly due to the lack of appropriate *in vitro* models and the fact that clinical trials are not usually performed in pediatric patients (Bjorkman 2006). Neonatal patients seem to be particularly susceptible to ADRs due to diminished clearance capacities in the first two years of life (Fabiano, Mameli et al. 2012). It is well-established that the neonatal liver is not fully developed at birth and undergoes a period of postnatal maturation, during which metabolic function is not comparable to that of adults. Drug metabolism by CYPs, in particular, varies greatly during the first two years after birth due to the ontogenic regulation of CYP gene expression (Hines 2008). Most drug-metabolizing CYPs, including CYP3A4, 2C19,

and 2C29, are expressed at low levels during gestation, at birth, and during early postnatal life, and do not reach expression levels comparable to that of adults until at least two years of age (Treluyer, Gueret et al. 1997, de Wildt, Kearns et al. 1999). This causes a diminished capacity for the metabolism of many drugs and is implicated in numerous ADRs in infants (Pearce, Gotschall et al. 2001, Hines 2013). Other enzymes, such as CYP3A7, are only expressed in the fetal and early postnatal liver and become undetectable once the liver is fully matured (Lacroix, Sonnier et al. 1997).

Whereas the postnatal ontogeny of CYPs in humans has been established, the induction of CYPs in response to drug treatment has not been well studied in pediatric populations at different stages of early development. It is largely unknown to what extent CYP activity can be induced in neonates and children compared to adults. Whether the capacity for enzymatic induction varies at different ages during postnatal liver maturation is also not understood. Several studies have additionally suggested neonatal exposures to inducer drugs, particularly the antiepileptic drug (AED) phenobarbital, can cause permanent alterations to expression and activities of CYPs in adult rodents (Agrawal and Shapiro 1996, Agrawal and Shapiro 2005, Tien, Liu et al. 2015, Piekos, Pope et al. 2017, Tien, Piekos et al. 2017). There also appears to be a "window of sensitivity" during neonatal life that allows the imprinting of lasting changes to CYP expression following treatment (Tien, Liu et al. 2015). This effect has not yet been validated with other small molecule drugs.

The goal of this work was to further examine the postnatal liver's capacity for CYP induction in response to inducer treatment at different ages spanning neonatal, infant, and adolescent stages in mice. This is a continuation of our previous studies that investigated the effects of neonatal phenobarbital treatment on expression of CYPs in adult mice. Whereas no animal model is a

perfect representation of human drug metabolism, the mouse is a useful *in vivo* system for studying developmental responses to drug treatment in a relatively short amount of time and for establishing proof-of-concepts prior to human pharmacokinetic studies (Turpeinen, Ghiciuc et al. 2007). Both short- and long-term effects of a single phenytoin dose on CYP expression and function were investigated, utilizing the novel sequential window acquisition of all theoretical mass spectra (SWATH-MS) method to quantify protein concentrations. Phenytoin was selected as an inducer because, like phenobarbital, it is an AED commonly utilized to treat neonatal seizures and a potent inducer of drug-metabolizing CYPs (Wang, Faucette et al. 2004, Jackson, Ferguson et al. 2006, Zeller and Giebe 2015). Based on previous studies, we hypothesized the neonatal liver is particularly sensitive to CYP induction by drug treatment and early life phenytoin exposure causes permanent alterations to CYP metabolism in adulthood.

Materials and Methods

Chemicals and Reagents. Phosphate buffered saline (PBS), 5,5-diphenylhydantoin salt (phenytoin, PHY), trifluoroacetic acid (TFA), formic acid, and acetonitrile were purchased from Sigma-Aldrich (St. Louis, MO). Urea and dithiothreitol (DTT) were obtained from Fisher Scientific Co. (Pittsburgh, PA). Iodoacetamide (IAA) and ammonium bicarbonate were purchased from Acros Organics (Morris Plains, NJ). TPCK-treated trypsin was obtained from Worthington Biochemical Corporation (Freehold, NJ). Bovine serum albumin (BSA) standard was purchased from Thermo Fisher Scientific (Waltham, MA).

Animals. C57Bl/6 mice (Jackson Laboratories, Bar Harbor, ME) were housed in accordance with the animal care guidelines outlined by the American Association for Animal Laboratory Sciences and were bred under standard conditions in the Animal Resources Facility at the University of Connecticut. The use of these animals was approved by the University of Connecticut's Institutional Animal Care and Use Committee. At 12 weeks of age, mice were set up into breeding pairs. To study short-term effects of drug treatment at different ages during postnatal development, mice were administered a single dose of phenytoin (100 mg/kg) or phosphate buffered saline (PBS) vehicle control intraperitoneally at ages of day 5, 10, 15, 20, 30, or 60 following birth. Twenty-four hours after the treatment, mice were sacrificed and liver samples were collected. To study long-term effects of drug treatment, mice at age of day 5 after birth were administered either phenytoin (100 mg/kg) or PBS vehicle control intraperitoneally. Following treatment, mice were sacrificed at different ages (day 10, 15, 20, 30, or 60 after birth) and livers were collected. Livers with gallbladders removed were snap frozen in liquid nitrogen then stored at -80°C. In both the short-term and long-term studies, 4-6 livers were collected at each age for both control and treatment groups. Both male and female mice were included in this study.

DMD Fast Forward. Published on June 8, 2018 as DOI: 10.1124/dmd.118.080861
This article has not been copyedited and formatted. The final version may differ from this version.

Total RNA extraction, reverse transcription, and RT-PCR. Total RNAs were isolated from whole livers using TRIzol reagent according to the manufacturer's protocol (Life Technologies, Guilford, CT). RNA concentrations were measured using a NanoDrop spectrophotometer (NanoDrop Technologies, Wilmington, DE) at a wavelength of 260 nm. To obtain cDNA, reverse transcription was performed using an iScript Reverse Transcription Supermix according to the manufacturer's protocol (Bio-Rad, Hercules, CA). RT-PCR was performed using a CFX-96 thermocycler system (Bio-Rad, Hercules, CA) with TaqMan gene expression assays for GAPDH, CYP3A16, 3A11, 2B10, and 2C29 (Thermo Fisher Scientific, Waltham, MA). Fold changes of CYP expression in phenytoin treated group compared to the PBS control group at each postnatal age were calculated using the $2^{-\Delta\Delta Ct}$ method described by Livak and Schmittgen (Livak and Schmittgen 2001) with a normalization of CYP expression to GAPDH. A consistent expression level of GAPDH is observed by either RNA-Seq or RT-PCR in mouse liver during postnatal maturation (Supplemental Figure 1).

Protein sample preparation and LC-MS/MS-based quantification. Whole mouse livers were chopped into small pieces using scissors and homogenized in PBS (pH 7.4) by a tissue grinder equipped with a Teflon pestle on ice. Liver S9 fractions were obtained by centrifuging the homogenate at 4°C at 10,000 g for 30 min. The supernatant containing the S9 fractions was transferred to a Beckman ultracentrifuge tube and centrifuged at 300,000 g for 20 min. The liver microsomes were obtained by re-suspending the pellet with PBS using the tissue grinder. Protein concentration was determined using a Pierce BCA protein assay kit (Thermo Fisher Scientific). Protein digestion was conducted according to a previously reported Lys-C/Trypsin combinatorial digestion protocol (Glatter, Ludwig et al. 2012) with minor modifications. An aliquot of 80 μg liver microsomal protein was mixed with the internal standard bovine serum albumin (BSA, 0.2

μg). After adding a 10-fold volume of pre-cooled acetone, the mixture was incubated at -20 °C for 2 hours and centrifuged. The supernatants were removed and the precipitated proteins were washed with 80% ethanol and then air-dried at room temperature. Proteins were resuspended in 4 mM DDT in 8 M urea solution containing 100 mM ammonium bicarbonate. Samples were sonicated and then incubated at 37 °C for 45 min. After samples were cooled down to room temperature, 20 mM IAA in 8 M urea/100 mM ammonium bicarbonate was added and incubated for 30 min at room temperature for alkylation. Following incubation, the urea concentration was adjusted to 6 M by adding 61.6 μL of 50 mM ammonium bicarbonate. Lysyl endopeptidase (Wako Chemicals, Richmond, VA) was added at an enzyme-to-protein ratio of 1:100 for the first step protein digestion for 6 hours at 37 °C. Samples were diluted to 1.6 M urea followed by a second digestion with trypsin at an enzyme-to-protein ratio of 1:50 for an overnight incubation at 37 °C. Digestion was terminated by adding 1 μL TFA.

Digested peptides were extracted and purified using Waters Oasis HLB columns (Waters Corporation, Milford, MA) according to the manufacturer's instructions. Eluted peptides were dried in a Speed Vac SPD1010 (Thermo Scientific, Hudson, NH) and reconstituted in 3% acetonitrile with 0.1% formic acid. The peptide samples were centrifuged and half of the supernatant was collected and supplemented with synthetic iRT standard solutions (Biognosys AG, Cambridge, MA) prior to LC-MS/MS analysis.

Peptides were analyzed in a TripleTOF 5600+ mass spectrometer (AB Sciex, Framingham, MA) coupled with an Eksigent 2D plus LC system (Eksigent Technologies, Dublin, CA). LC separation was performed via a trap-elute configuration, which included a trapping column (ChromXP C18-CL, 120 Å, 5 μm, 0.3 mm cartridge, Eksigent Technologies, Dublin, CA) and an analytical column (ChromXP C18-CL, 120 Å, 150 x 0.3 mm, 5 μm, Eksigent Technologies,

Dublin, CA). The mobile phase consisted of water with 0.1% formic acid (phase A) and acetonitrile with 0.1% formic acid (phase B) (Avantor, Center Valley, PA). A total of 6 μg protein was injected for analysis. Peptides were trapped and cleaned on the trapping column with phase A delivered at a flow rate of 10 μL/min for 3 min followed by separation on the analytical column with a gradient elution at a flow rate of 5 μL/min. The gradient time program was set as follows for phase B: 0 to 68 min: 3% to 30%, 68 to 73 min: 30% to 40%, 73 to 75 min: 40% to 80%, 75 to 78 min: 80%, 78 to 79 min: 80% to 3%, and finally 79 to 90 min at 3% for column equilibration. The TripleTOF instrument was operated in a positive ion mode with an ion spray voltage floating at 5500 v, ion source gas one at 28 psi, ion source gas two at 16 psi, curtain gas at 25 psi, and source temperature at 280 °C.

To generate the reference spectral library for SWATH data analysis, Information-Dependent Acquisition (IDA) was performed for three pooled mouse liver microsomes samples with equal protein amounts. The IDA method included a 250 ms TOF-MS scan from 400 to 1250 Da, followed by an MS/MS scan in high sensitivity mode from 100 to 1500 Da (50 ms accumulation time, 10 ppm mass tolerance, charge state from +2 to +5, rolling collision energy and dynamic accumulation) of the top 30 precursor ions from the TOF-MS scan. The IDA data from the pooled mice liver microsomes were searched by MaxQuant (version 1.5.3.30, Max Planck Institute of Biochemistry, Germany). The mouse FASTA file with 16,911 protein entries was downloaded from Uniport on 8/29/2016 and was used as the reference sequences for search with trypsin/P as the protease. Peptide length was set between 7 and 25 residues with up to two missed cleavage sites allowed. Carbamidomethyl (C) was set as a fixed modification. A false discovery rate of 0.01 was used as the cutoff for both peptide and protein identification.

All microsomes samples were analyzed using a SWATH method with the "SWATH (VW 100)" isolation scheme, which comprised of a 250 ms TOF-MS scan from 400 to 1250 Da, followed by MS/MS scans from 100 to 1500 Da performed on all precursors in a cyclic manner. The accumulation time was 50 ms per isolation window, resulting in a total cycle time of 2.8 s. The spectral alignment and target data extraction of the SWATH data were performed on Skyline-daily (version 3.7.1.11271, University of Washington, Seattle, WA) with the reference spectral library generated from the aforementioned IDA searches. The MS1 and MS/MS filtering were both set as "TOF mass analyzer" with the resolution power of 30,000 and 15,000, respectively. The retention time prediction was based on the auto-calculate regression implemented in the iRT calculator. Proper peak selection was reviewed manually with the automated assistance of Skyline-daily. The surrogate peptides used for the quantification of CYP2B10, 2C29, 3A11, and 3A16 proteins are listed (Supplemental Table 1). The selections were based on the uniqueness and chromatographic performance of these peptides. The peak areas of top 3 to 5 fragment ions were summed up and normalized to the internal standard BSA. The BSA-normalized peak area of each peptide was further divided by the average peak area of the 30 samples to calculate the relative abundance of the peptide. The average of relative abundance of all surrogate peptides of a protein was used to determine protein relative abundance.

Evaluation of enzymatic activities. Liver tissues were homogenized in ice-cold 100 mM PBS (pH 7.4) and S9 fractions were obtained by centrifugation. Protein concentrations were determined using a Pierce BCA protein assay kit (Thermo Fisher Scientific, Rockford, IL). Pentoxyresorufin O-dealkylation, paclitaxel 6-hydroxylation, and midazolam 1'-hydroxylation, were used as probes for 2B10 (Lam, Jiang et al. 2010), 2C29 (Gustafson, Long et al. 2005), and CYP3A11 (Lam, Jiang et al. 2010) activities, respectively. Incubations were carried out in 100 mM phosphate-buffered

saline (pH 7.4), containing 0.1 mg of mouse liver S9 protein and 30 µM substrate for a final volume of 95 µL. The reactions were initiated by adding 5 µL of 20 mM NADPH and continued for 30 min for pentoxyresorufin and paclitaxel or 10 min for midazolam. Incubations were terminated by adding 100 µL of ice-cold acetonitrile.

After centrifugation at 15,000 rpm, a 1.0 µL aliquot was injected into a Waters Synapt G2-S QTOFMS system (Milford, MA) for metabolite quantification analysis. Chromatographic separation of metabolites was performed on an Acquity UPLC BEH C18 column (2.1 × 50 mm, 1.7 µm, Waters). The mobile phase A (MPA) consisted of 0.1 % formic acid in water and mobile phase B (MPB) was 0.1% formic acid in acetonitrile. The gradient for aqueous extraction began at 5% MPB and held for 0.5 min, followed by 5 min linear gradient to 95% MPB, held for 2 min, and decreased to 5% MPB for column equilibration. The flow rate of the mobile phase was 0.50 mL/min and the column temperature was maintained at 50 °C. The G2-S QTOFMS system was operated in resolution mode (resolution ~20,000) with electrospray ionization. The source and desolvation temperatures were set at 150 and 500 °C, respectively. Nitrogen was applied as the cone gas (50 L/hr) and desolvation gas (800 L/hr). The capillary and cone voltages were set at 0.8 kV and 40 V. The data were acquired in positive ionization mode. QTOFMS was calibrated with sodium formate and monitored by the intermittent injection of lock mass leucine encephalin (*m/z* = 556.2771) in real time. Quanlynx software (Waters, Milford, MA) was used for the quantification of the concentration of metabolites.

Enzyme reactions were validated to be linear over the 30 min incubation periods. The linear ranges of detection for resorufin, 1'hydroxymidazolam, and hydroxytaxol were 1-300 ng/ml, 0.2-200 mg/ml, and 8-1000 ng/ml, respectively.

Statistical Analysis. Data are presented as the mean ± S.E (standard error). Statistical analyses were performed using GraphPad Prism 7 Software (GraphPad Software, Inc., La Jolla, CA). Comparisons between groups were done using Student's *t*-test and were determined using the two-stage linear step-up procedure of Benjamini, Krieger, and Yekutieli with Q = 1%. A value of $p < 0.05$ was considered to be significant.

Results

To evaluate the impact of phenytoin exposure on the expression and function of drug-metabolizing CYPs throughout postnatal maturation, a mouse model was utilized. Short-term effects of drug treatment were evaluated at 24 hours following administration of a single dose of phenytoin in mice at different ages. Long-term effects of drug treatment were evaluated by administering a single dose of phenytoin at age of day 5 after birth, then collecting livers at different time points throughout development, beginning at age of day 10. When comparing mouse to human ages, 9 days in the mouse has been compared to 1 year in the human when considering total lifespans. Additionally, mice are weaned between days 21-28 of age, while humans are weaned between 6-12 months of age (Dutta and Sengupta 2016). Based on this, the age of day 5 in mouse would correlate with roughly the first 3-6 months of life in humans when hepatic CYP expression is known to be rapidly changing. The expression of hepatic murine CYP2B10, 2C29, 3A11, and 3A16 enzymes were evaluated as representative members of the CYP2B, 2C, and 3A subfamilies that are known to be involved in the metabolism of xenobiotics and drugs across species (Martignoni, Groothuis et al. 2006). The effect of drug treatment on each enzyme was measured at the mRNA level using RT-PCR, at the protein level using SWATH-MS quantification, and at the enzymatic activity level using *in vitro* CYP probe substrates and LC-MS quantification. SWATH-MS is a relatively novel method for measuring protein concentrations, but previous studies have suggested lower limits of peptide quantitation in the 0.1 to 10 fmol range (Collins, Hunter et al. 2017). Both male and female mice were evaluated collectively for data presented at ages younger than day 30, however male and female data were evaluated separately at age of day 60. At each time point, mice that received drug treatment were compared against age-matched mice that received a vehicle control.

DMD Fast Forward. Published on June 8, 2018 as DOI: 10.1124/dmd.118.080861
This article has not been copyedited and formatted. The final version may differ from this version.

Effects of phenytoin exposure on CYP2B10 expression, induction, and function throughout postnatal maturation. The fold-increase of CYP2B10 mRNA induction 24 hours following phenytoin administration was the greatest of all CYPs measured, however the large value for fold-induction may be overstated due to low basal expression of CYP2B10 in the liver compared to other enzymes (Fig. 1A). Mice at age of day 10 showed the greatest fold-change in mRNA expression when compared to control, whereas fold-changes at other ages were more comparable to those observed in adult mice following phenytoin treatment. Adult males also had higher fold changes than females at day 60; however, adult male mice are known to have lower basal CYP2B10 expression than females. When comparing gene expression to GAPDH, which was unaffected by phenytoin treatment, CYP2B10 mRNA was much less abundant than GAPDH in control mice but reached similar levels following drug exposure (Fig. 1B). The surge in CYP2B10 expression at age of day 30 was also apparent and was associated with a spike in the inducibility of the enzyme.

CYP2B10 protein was also quantified 24 hours after treatment in neonatal mice at age of day 5 and adult male mice at age of day 60 (Fig. 1C). Following vehicle treatment, CYP2B10 protein was nearly undetectable in both neonates and adults; however, significant induction of protein was evident at both ages following phenytoin treatment. The inductive potential was far greater in adults than in neonates, however induced levels of CYP2B10 in the neonate significantly exceeded basal levels in the adult. This observation was also reflected in a CYP2B10 enzyme activity assay determined by pentoxyresorufin O-dealkylation in S9 fractions prepared from neonatal and adult liver samples (Fig. 1D), indicating functional consequences of induction by phenytoin.

DMD Fast Forward. Published on June 8, 2018 as DOI: 10.1124/dmd.118.080861
This article has not been copyedited and formatted. The final version may differ from this version.

The long-term effects of phenytoin treatment on CYP2B10 were examined using the same techniques. Mice at age of day 5 were all administered a single dose of phenytoin or vehicle control and were allowed to age to designated time points. Livers were then collected and effects on CYP2B10 mRNA and protein expression were evaluated. Five days following phenytoin treatment, CYP2B10 mRNA was still significantly induced at age of day 10 compared to mice that received vehicle (Fig. 1E). No other significant alterations were observed in CYP2B10 mRNA expression until the mice reached age of day 60. However, the increased expression was only observed in males and to a smaller extent than the fold change observed at day 10. This long-term effect was not reflected at the protein (Fig. 1F) or enzymatic activity (Fig. 1G) levels, however, as there were no significant differences in CYP2B10 protein or pentoxyresorufin O-dealkylation in adult male mice that received phenytoin treatment at age of day 5.

Effects of phenytoin exposure on CYP2C29 expression and induction throughout postnatal maturation. Induction of CYP2C29 mRNA and protein expression 24 hours following phenytoin treatment was also examined at different ages. The amount of mRNA was significantly greater in mice that received phenytoin compared to mice that received vehicle at all ages tested, with age of day 10 appearing to again be the most sensitive to enzyme induction (Fig. 2A). When evaluating CYP2C29 mRNA expression relative to GAPDH expression, CYP2C29 mRNA was much less abundant in neonates at age of day 5 in PBS treated control mice, but steadily increased to levels comparable to GAPDH at day 20 (Fig. 2B). Induced levels of CYP2C29 mRNA exceeded GAPDH expression by around 10-fold at all ages except day 5, where it remained minimally expressed. This was also reflected in CYP2C29 protein quantified at age of day 5 following a 24-hour exposure duration to phenytoin (Fig. 2C). Phenytoin-mediated protein induction at age of day 5 was significant, but minimal compared to induction at the adult age of day 60. Induced levels of

DMD Fast Forward. Published on June 8, 2018 as DOI: 10.1124/dmd.118.080861
This article has not been copyedited and formatted. The final version may differ from this version.

CYP2C29 protein in the neonate were significantly lower than even basal levels of the protein in the adult. Enzymatic activity of CYP2C29 could not be evaluated in these experiments due to not insufficient protein isolated from prepared microsomes.

Long-term effects of neonatal phenytoin exposure on CYP2C29 expression at later ages were not apparent. Following day 5 administration of phenytoin, there were no persisting alterations to CYP2C29 mRNA (Fig. 2D) in adulthood when compared to control mice. There appeared to be significant up-regulation of CYP2C29 mRNA in treated mice at ages of day 20 and 30; however, the fold-change in gene expression may not be sufficient enough to produce biological consequences. Interestingly, CYP2C29 protein expression was lower in adult mice that received phenytoin as neonates (Fig. 2E); however, we could not further determine whether this would translate into a functional decrease in CYP2C29 metabolic activity.

Effects of phenytoin exposure on CYP3A11 expression, induction, and function throughout postnatal maturation. The short-term effects on CYP3A11 mRNA induction following phenytoin treatment were evident across all ages studied during postnatal development. The greatest fold-change between phenytoin-treated mice and control mice occurred in neonates at age of day 5, presumably because this is when the basal expression of CYP3A11 is the lowest (Fig. 3A). As mice matured following birth, basal expression of CYP3A11 mRNA increased along with increased induced levels of mRNA with age (Fig. 3B). Maximal induction occurred at adult ages (day 30 and 60), which was also reflected in the expression of CYP3A11 protein (Fig. 3C). Protein quantification revealed that induced levels of CYP3A11 in the neonate at age of day 5 were not statistically different from basal levels of CYP3A11 protein in the adult. This was also confirmed by enzymatic activity analyses with midazolam in liver S9 fractions (Fig. 3D). At age of day 5, mice treated with phenytoin had similar rates of 1-hydroxymidazolam metabolite

formation as adult mice treated with vehicle control, while adult mice treated with phenytoin produced the most metabolite overall.

There also appeared to be no significant effects on CYP3A11 expression or function in the long-term following neonatal phenytoin exposure. Following administration at day 5, phenytoin seemed to increase the range of CYP3A11 mRNA expression at later ages between mice, such as at age day 10 where the standard error in the fold changes of treated mice was larger than in control mice. However, there were no significant differences in the mean expression from control mice, except for a slight increase at age day 30 (Fig. 3E). This was also confirmed in protein (Fig. 3F) and enzymatic activity (Fig. 3G) quantification. At the adult ages, there were no significant differences in mice that received phenytoin at age of day 5 of CYP3A11 protein expression or midazolam metabolism.

Effect of phenytoin exposure on the postnatal repression of the fetal enzyme CYP3A16. CYP3A16 is considered to be the fetal enzyme of the CYP3A subfamily of enzymes. While it is highly expressed immediately after birth, its expression declines steadily throughout postnatal maturation and is undetectable in the adult liver. Phenytoin treatment also appeared to significantly affect short-term CYP3A16 expression at different ages during postnatal development. Twenty-four hours after phenytoin administration, CYP3A16 mRNA was significantly suppressed in mice at all ages examined (Fig. 4A). The fold-change in the decrease of expression was greatest at age day 20 and this corresponded to the age in which CYP3A16 mRNA became undetectable in phenytoin-treated mice (Fig. 4B). CYP3A16 mRNA was not detected by RT-PCR in mice at ages of day 30 or 60, so the data are not shown. The decrease in CYP3A16 in response to phenytoin treatment was also confirmed by protein quantification (Fig. 4C). At age of day 5, CYP3A16

protein was decreased following drug exposure, however not significantly. CYP3A16 protein was not detected in adults regardless of phenytoin administration.

Discussion

The present study reveals both the immediate and persistent effects on the expression and functions of several drug-metabolizing CYP enzymes following exposure to the antiepileptic drug phenytoin during murine postnatal development. Short-term induction of CYP2B10, 2C29, and 3A11 after phenytoin administration for 24 hours seems to vary in extent based on age and sex. Younger pups, such as those at ages of day 5 and day 10, had higher fold changes relative to control for CYP induction; however, these values may be overstated due to the low basal expression of CYPs in the neonatal period. With increasing age, the values for fold induction decreased compared to control animals. Based on this, it is unclear how induced levels of each enzyme change independent of their basal expression levels. For this reason, we also chose to evaluate mRNA expression of each CYP relative to GAPDH. GAPDH expression was not altered by drug treatment and remained relatively consistent throughout postnatal development. Analyzing gene expression in relation to GAPDH allowed the ontogeny of each CYP enzyme to be observed in basal and induced states at each age. Induction of each enzyme (CYP2B10, 2C29, and 3A11) appeared to be qualitatively proportional to the basal expression level of the enzyme; the higher the mRNA expression of a CYP at a certain age, the greater its induction capacity. On the other hand, CYP3A16 appeared to be repressed to greater extents at increasing ages, which correlated with decreasing basal expression.

For both CYP2B10 and 2C29, day 10 appeared to be the age most sensitive to the inductive effects of phenytoin as evidenced by the greatest fold changes in mRNA expression compared to control mice. Interestingly, this correlates with our previous data that shows a surge of CYP2B10 and 2C29 expression beginning at the same age (Peng, Yoo et al. 2012). Both of these enzymes are primarily under the transcriptional control of the constitutive androstane nuclear receptor

(CAR), while CYP3A11 is known to be regulated primarily by the pregnane X nuclear receptor (PXR). The expression of PXR and CAR actually appear to be the highest during early postnatal life in both mouse and infant humans (Vyhlidal, Gaedigk et al. 2006, Gunewardena, Yoo et al. 2015). The consequences of elevated expression of these nuclear receptors at the neonatal stage in the expression and regulation of CYPs are not understood.

The inducibility of other hepatic drug processing genes utilizing direct activation of PXR and CAR has also shown to be age-dependent in mouse (Li, Renaud et al. 2016). Greater fold changes in RNA expression following xenobiotic treatment are typically observed at the neonatal age. However, our study shows that despite the apparent greater extent of RNA induction at younger ages, protein expression and enzymatic activity following phenytoin treatment is still greater in adults than neonates. The expression of CYP2B10, 2C29, and 3A11 proteins is several magnitudes higher in adults than in neonates following phenytoin treatment, suggesting the adult liver has a greater capacity for enzyme induction following drug treatment than the infant liver. In the case of CYP2B10, protein expression in the neonate following phenytoin exposure exceeds that of adults in basal conditions with vehicle treatment. The expression of CYP2C29 protein following phenytoin treatment in the neonate, however, does not reach adult expression levels. This data suggests that induction in response to drug treatment is not equivalent in neonatal and adult mice, even following the same dose, and adult data cannot be extrapolated to younger ages. Only liver samples from day 5 were used for protein and enzymatic activity analyses of early life, so additional ages will need to be examined in the future.

Previous work from our laboratory has defined the ontogenic profiles of all CYPs in the mouse liver from two days before birth through day 60 after birth (Hart et al., 2009; Peng et al., 2012). The expression pattern of the murine enzymes investigated in this study, namely CYP2B10, 2C29,

3A11, and 3A16, follow specific ontogenic patterns throughout postnatal maturation, and our data shows that induction varies depending on developmental age as well. A better understanding of the mechanisms regulating enzyme induction between the developing and fully mature mouse liver are needed to understand this observation. The expression of CYPs in the human fetal, neonatal, and infant liver also follow distinct ontogenic patterns that may be specific to each enzyme. However, there are still marked differences between human and mouse CYP-mediated metabolism, especially in terms of enzyme induction and regulation. Other studies have also highlighted the need for pediatric pharmacokinetics to be evaluated in age- and maturation-dependent models, rather than grouping all neonatal and infant guidelines into one pediatric category (Suzuki, Mimaki et al. 1994, Abduljalil, Jamei et al. 2014).

The long-term effects of neonatal phenytoin exposure were also investigated in our study. Following day 5 administration, CYP2B10 was the only CYP that remained overexpressed at day 10. This mechanism will have to be further elucidated, as the half-life of phenytoin in adult mice is only 16 hours (Markowitz, Kadam et al. 2010), however this might not be true for neonates. At day 60, there appears to be slight, but significant, overexpression of CYP3A11 and CYP2B10 RNA in male mice only. However, the induction was not observed in the protein or enzymatic activity analyses. Interestingly, CYP2C29 protein expression is significantly down-regulated at day 60 following neonatal phenytoin exposure, despite no significant changes observed at the mRNA level.

Additional studies will be necessary to further distinguish why neonatal exposure to phenobarbital produces overexpression of CYP mRNA, protein, and function in adulthood, while exposure to phenytoin does not. Phenobarbital upregulates the transcription of CYPs through its indirect action on the nuclear receptor CAR (Wei, Zhang et al. 2000). Previous work has shown

DMD Fast Forward. Published on June 8, 2018 as DOI: 10.1124/dmd.118.080861
This article has not been copyedited and formatted. The final version may differ from this version.

that direct activation using 1,4-bis[2-(3,5-dichloropyridoyloxy)] benzene (TCPOBOP), a murine-specific CAR ligand, at the neonatal age also produces permanent alterations to CYP expression (Li, Cheng et al. 2016) and function in adulthood, which alters the efficacy of zoxazolamine administered later in life (Chen, Fu et al. 2012). Phenobarbital exposure at the neonatal age also caused a decrease in efficacy of omeprazole administered to adult mice, suggesting its role in a possible non-conventional DDI (Tien, Piekos et al. 2017). Due to phenytoin's ability to cause CAR activation, we presumed that neonatal exposure would also cause a similar permanent alteration to CYP expression; however, this was not the case. Unlike TCPOBOP, both phenobarbital and phenytoin produce CAR activation indirectly. While they both are AEDs, these chemicals have different mechanisms of action for treating seizures. It is plausible that phenobarbital and phenytoin produce indirect CAR activation via separate mechanisms or pathways, and a pathway further upstream of CAR activation is what becomes permanently affected following neonatal phenobarbital treatment that is not impacted by phenytoin treatment.

Phenytoin and phenobarbital are both considered first-line therapy for treating seizures in neonates with phenobarbital appearing to be slightly more efficacious (Painter, Scher et al. 1999, Booth and Evans 2004, Pathak, Upadhyay et al. 2013). Both drugs have indications for acute treatment of infant seizures as well as chronic administration for control of epileptic disorders in infants and children. Phenytoin therapy, as with most other AEDs, is initiated with a larger loading dose (18-20 mg/kg for pediatric use), followed by subsequent lower maintenance doses for recurrent seizure control. Appropriate doses are calculated based on the patient's body weight, however it is unclear whether other factors are taken into account (Hawcutt, Sampath et al. 2011). In the current study, we administered mice a single dose of 100 mg/kg phenytoin, which is equivalent to a human dose of 8 mg/kg according to the FDA's Guidance for Industry to

extrapolate human dose concentrations from animal data. This is likely more representative of a maintenance dose of phenytoin; however, this was the maximal dose we could achieve while avoiding excessive toxicity. Perhaps a higher dosing concentration, or multiple-day phenytoin treatment, would have produced the permanent overexpression of CYPs that was observed with phenobarbital treatment.

Phenytoin has a narrow therapeutic index with a large propensity to produce ADRs due to patient interindividual variability. Adverse side effects of phenytoin are common and often include rashes, headache, behavioral changes, Steven-Johnson syndrome, cardiovascular collapse, and arrhythmias, especially with a rapid intravenous administration, in both children and adults (Bansal, Azad et al. 2013, Polat, Karaoglu et al. 2015). Many pediatric patients with severe epilepsy are often treated with polytherapy, and interactions between phenytoin and other AEDs and the resulting adverse effects have been documented. For example, concurrent treatment with phenytoin and valproic acid produced phenytoin toxicity in an adolescent epileptic patient, despite adhering to pediatric dosing guidelines for phenytoin (Carvalho, Carnevale et al. 2014). A better understanding of the mechanism behind phenytoin-mediated CYP induction via CAR, especially through postnatal development, could help alleviate the high-risk of ADRs that commonly accompany phenytoin treatment. Despite the high-risk of potentially dangerous side effects, phenytoin might be a better therapeutic option for seizure control in infants, as it may not produce the permanent effects on CYP expression and liver function caused by phenobarbital. This data warrants further studies in humans.

Authorship Contributions

Participated in research design: Piekos, Zhong, Ma, and Zhu.

Conducted experiments: Piekos, Chen, Wang, Shi, Yaqoob.

Contributed new reagents or analytic tools: n/a.

Performed data analysis: Piekos, Wang, Shi, Ma, Zhu, and Zhong.

Wrote or contributed to the writing of the manuscript: Piekos, Zhong, Ma, and Zhu.

References

Abduljalil, K., M. Jamei, A. Rostami-Hodjegan and T. N. Johnson (2014). "Changes in individual drug-independent system parameters during virtual paediatric pharmacokinetic trials: introducing time-varying physiology into a paediatric PBPK model." AAPS J **16**(3): 568-576.

Agrawal, A. K. and B. H. Shapiro (1996). "Imprinted overinduction of hepatic CYP2B1 and 2B2 in adult rats neonatally exposed to phenobarbital." J Pharmacol Exp Ther **279**(2): 991-999.

Agrawal, A. K. and B. H. Shapiro (2005). "Neonatal phenobarbital imprints overexpression of cytochromes P450 with associated increase in tumorigenesis and reduced life span." FASEB J **19**(3): 470-472.

Bansal, D., C. Azad, M. Kaur, N. Rudroju, P. Vepa and V. Guglani (2013). "Adverse effects of antiepileptic drugs in North Indian pediatric outpatients." Clin Neuropharmacol **36**(4): 107-113.

Bjorkman, S. (2006). "Prediction of cytochrome p450-mediated hepatic drug clearance in neonates, infants and children : how accurate are available scaling methods?" Clin Pharmacokinet **45**(1): 1-11.

Booth, D. and D. J. Evans (2004). "Anticonvulsants for neonates with seizures." Cochrane Database Syst Rev(4): CD004218.

Carvalho, I. V., R. C. Carnevale, M. B. Visacri, P. G. Mazzola, R. de Fatima Lopes Ambrosio, M. C. dos Reis, R. A. de Queiroz and P. Moriel (2014). "Drug interaction between phenytoin and valproic acid in a child with refractory epilepsy: a case report." J Pharm Pract **27**(2): 214-216.

Chen, W. D., X. Fu, B. Dong, Y. D. Wang, S. Shiah, D. D. Moore and W. Huang (2012). "Neonatal activation of the nuclear receptor CAR results in epigenetic memory and permanent change of drug metabolism in mouse liver." Hepatology **56**(4): 1499-1509.

Collins, B. C., C. L. Hunter, Y. Liu, B. Schilling, G. Rosenberger, S. L. Bader, D. W. Chan, B. W. Gibson, A. C. Gingras, J. M. Held, M. Hirayama-Kurogi, G. Hou, C. Krisp, B. Larsen, L. Lin, S. Liu, M. P. Molloy, R. L. Moritz, S. Ohtsuki, R. Schlapbach, N. Selevsek, S. N. Thomas, S. C. Tzeng, H. Zhang and R. Aebersold (2017). "Multi-laboratory assessment of reproducibility,

qualitative and quantitative performance of SWATH-mass spectrometry." Nat Commun **8**(1): 291.

Dai, D., J. A. Feinstein, W. Morrison, A. F. Zuppa and C. Feudtner (2016). "Epidemiology of Polypharmacy and Potential Drug-Drug Interactions Among Pediatric Patients in ICUs of U.S. Children's Hospitals." Pediatr Crit Care Med **17**(5): e218-228.

de Wildt, S. N., G. L. Kearns, J. S. Leeder and J. N. van den Anker (1999). "Cytochrome P450 3A: ontogeny and drug disposition." Clin Pharmacokinet **37**(6): 485-505.

Dutta, S. and P. Sengupta (2016). "Men and mice: Relating their ages." Life Sci **152**: 244-248.

Fabiano, V., C. Mameli and G. V. Zuccotti (2012). "Adverse drug reactions in newborns, infants and toddlers: pediatric pharmacovigilance between present and future." Expert Opin Drug Saf **11**(1): 95-105.

Glatter, T., C. Ludwig, E. Ahrne, R. Aebersold, A. J. Heck and A. Schmidt (2012). "Large-scale quantitative assessment of different in-solution protein digestion protocols reveals superior cleavage efficiency of tandem Lys-C/trypsin proteolysis over trypsin digestion." J Proteome Res **11**(11): 5145-5156.

Gunewardena, S. S., B. Yoo, L. Peng, H. Lu, X. Zhong, C. D. Klaassen and J. Y. Cui (2015). "Deciphering the Developmental Dynamics of the Mouse Liver Transcriptome." PLoS One **10**(10): e0141220.

Gustafson, D. L., M. E. Long, E. L. Bradshaw, A. L. Merz and P. J. Kerzic (2005). "P450 induction alters paclitaxel pharmacokinetics and tissue distribution with multiple dosing." Cancer Chemother Pharmacol **56**(3): 248-254.

Hart, S. N., Y. Cui, C. D. Klaassen and X. B. Zhong (2009). "Three patterns of cytochrome P450 gene expression during liver maturation in mice." Drug Metab Dispos **37**(1): 116-121.

Hawcutt, D. B., S. Sampath, A. Timmis, V. Newland, P. Newland and R. Appleton (2011). "Serum phenytoin concentrations in paediatric patients following intravenous loading." Arch Dis Child **96**(9): 883-884.

Hines, R. N. (2008). "The ontogeny of drug metabolism enzymes and implications for adverse drug events." Pharmacol Ther **118**(2): 250-267.

Hines, R. N. (2013). "Developmental expression of drug metabolizing enzymes: impact on disposition in neonates and young children." Int J Pharm **452**(1-2): 3-7.

Jackson, J. P., S. S. Ferguson, M. Negishi and J. A. Goldstein (2006). "Phenytoin induction of the cyp2c37 gene is mediated by the constitutive androstane receptor." Drug Metab Dispos **34**(12): 2003-2010.

Lacroix, D., M. Sonnier, A. Moncion, G. Cheron and T. Cresteil (1997). "Expression of CYP3A in the human liver--evidence that the shift between CYP3A7 and CYP3A4 occurs immediately after birth." Eur J Biochem **247**(2): 625-634.

Lam, J. L., Y. Jiang, T. Zhang, E. Y. Zhang and B. J. Smith (2010). "Expression and functional analysis of hepatic cytochromes P450, nuclear receptors, and membrane transporters in 10- and 25-week-old db/db mice." Drug Metab Dispos **38**(12): 2252-2258.

Li, C. Y., S. L. Cheng, T. K. Bammler and J. Y. Cui (2016). "Editor's Highlight: Neonatal Activation of the Xenobiotic-Sensors PXR and CAR Results in Acute and Persistent Down-regulation of PPARalpha-Signaling in Mouse Liver." Toxicol Sci **153**(2): 282-302.

Li, C. Y., H. J. Renaud, C. D. Klaassen and J. Y. Cui (2016). "Age-Specific Regulation of Drug-Processing Genes in Mouse Liver by Ligands of Xenobiotic-Sensing Transcription Factors." Drug Metab Dispos **44**(7): 1038-1049.

Lin, J. H. (2006). "CYP induction-mediated drug interactions: in vitro assessment and clinical implications." Pharm Res **23**(6): 1089-1116.

Livak, K. J. and T. D. Schmittgen (2001). "Analysis of relative gene expression data using real-time quantitative PCR and the 2(-Delta Delta C(T)) Method." Methods **25**(4): 402-408.

Markowitz, G. J., S. D. Kadam, D. M. Boothe, N. D. Irving and A. M. Comi (2010). "The pharmacokinetics of commonly used antiepileptic drugs in immature CD1 mice." Neuroreport **21**(6): 452-456.

Martignoni, M., G. M. Groothuis and R. de Kanter (2006). "Species differences between mouse, rat, dog, monkey and human CYP-mediated drug metabolism, inhibition and induction." Expert Opin Drug Metab Toxicol **2**(6): 875-894.

Painter, M. J., M. S. Scher, A. D. Stein, S. Armatti, Z. Wang, J. C. Gardiner, N. Paneth, B. Minnigh and J. Alvin (1999). "Phenobarbital compared with phenytoin for the treatment of neonatal seizures." N Engl J Med **341**(7): 485-489.

Palleria, C., A. Di Paolo, C. Giofre, C. Caglioti, G. Leuzzi, A. Siniscalchi, G. De Sarro and L. Gallelli (2013). "Pharmacokinetic drug-drug interaction and their implication in clinical management." J Res Med Sci **18**(7): 601-610.

Pathak, G., A. Upadhyay, U. Pathak, D. Chawla and S. P. Goel (2013). "Phenobarbitone versus phenytoin for treatment of neonatal seizures: an open-label randomized controlled trial." Indian Pediatr **50**(8): 753-757.

Pearce, R. E., R. R. Gotschall, G. L. Kearns and J. S. Leeder (2001). "Cytochrome P450 Involvement in the biotransformation of cisapride and racemic norcisapride in vitro: differential activity of individual human CYP3A isoforms." Drug Metab Dispos **29**(12): 1548-1554.

Peng, L., B. Yoo, S. S. Gunewardena, H. Lu, C. D. Klaassen and X. B. Zhong (2012). "RNA sequencing reveals dynamic changes of mRNA abundance of cytochromes P450 and their alternative transcripts during mouse liver development." Drug Metab Dispos **40**(6): 1198-1209.

Piekos, S., C. Pope, A. Ferrara and X. B. Zhong (2017). "Impact of Drug Treatment at Neonatal Ages on Variability of Drug Metabolism and Drug-drug Interactions in Adult Life." Curr Pharmacol Rep **3**(1): 1-9.

Polat, I., P. Karaoglu, M. Ayanoglu, U. Yis and S. Hiz (2015). "Life-Threatening and Rare Adverse Effects of Phenytoin." Pediatr Emerg Care **31**(7): e3.

Suzuki, Y., T. Mimaki, S. Cox, J. Koepke, J. Hayes and P. D. Walson (1994). "Phenytoin age-dose-concentration relationship in children." Ther Drug Monit **16**(2): 145-150.

Tien, Y. C., K. Liu, C. Pope, P. Wang, X. Ma and X. B. Zhong (2015). "Dose of Phenobarbital and Age of Treatment at Early Life are Two Key Factors for the Persistent Induction of Cytochrome P450 Enzymes in Adult Mouse Liver." Drug Metab Dispos **43**(12): 1938-1945.

Tien, Y. C., S. C. Piekos, C. Pope and X. B. Zhong (2017). "Phenobarbital Treatment at a Neonatal Age Results in Decreased Efficacy of Omeprazole in Adult Mice." Drug Metab Dispos **45**(3): 330-335.

Treluyer, J. M., G. Gueret, G. Cheron, M. Sonnier and T. Cresteil (1997). "Developmental expression of CYP2C and CYP2C-dependent activities in the human liver: in-vivo/in-vitro correlation and inducibility." Pharmacogenetics **7**(6): 441-452.

Turpeinen, M., C. Ghiciuc, M. Opritoui, L. Tursas, O. Pelkonen and M. Pasanen (2007). "Predictive value of animal models for human cytochrome P450 (CYP)-mediated metabolism: a comparative study in vitro." Xenobiotica **37**(12): 1367-1377.

Vyhlidal, C. A., R. Gaedigk and J. S. Leeder (2006). "Nuclear receptor expression in fetal and pediatric liver: correlation with CYP3A expression." Drug Metab Dispos **34**(1): 131-137.

Wang, H., S. Faucette, R. Moore, T. Sueyoshi, M. Negishi and E. LeCluyse (2004). "Human constitutive androstane receptor mediates induction of CYP2B6 gene expression by phenytoin." J Biol Chem **279**(28): 29295-29301.

Wei, P., J. Zhang, M. Egan-Hafley, S. Liang and D. D. Moore (2000). "The nuclear receptor CAR mediates specific xenobiotic induction of drug metabolism." Nature **407**(6806): 920-923.

Zanger, U. M. and M. Schwab (2013). "Cytochrome P450 enzymes in drug metabolism: regulation of gene expression, enzyme activities, and impact of genetic variation." Pharmacol Ther **138**(1): 103-141.

Zeller, B. and J. Giebe (2015). "Pharmacologic Management of Neonatal Seizures." Neonatal Netw **34**(4): 239-244.

Footnotes

This study was supported by the National Institute of General Medical Sciences [Grant R01GM-118367] (to X.B.Z); the American Foundation for Pharmaceutical Education (to S.C.P); the National Institute for Diabetes and Digestive and Kidney Diseases [Grant R01DK090305] (to X.M); the National Heart, Lung, and Blood Institute [Grant R01HL126969] (to H.J.Z). This study was also partly supported by the Institute for System Genomics at the University of Connecticut (to X.B.Z).

Figure Legends

Fig. 1. Effects of phenytoin treatment on the expression and activity of CYP2B10 at different ages during postnatal maturation. Male and female mice were treated with either vehicle control (PBS) or 100 mg/kg phenytoin (PHY) at different ages following birth. The short-term effects of PHY treatment were measured 24 hours after treatment. Changes in gene expression were evaluated at the mRNA level using RT-PCR, then fold-changes were calculated using the $2^{-\Delta\Delta Ct}$ method. Data points represent fold-changes in gene expression of individual mice treated with PBS or PHY compared to average ΔCt of mice that received PBS control (A). Ct values from RT-PCR experiments were also compared to the GAPDH Ct value in each individual mouse and the differences are expressed as $2^{-(Ct(CYP)-Ct(GAPDH))}$ (B). The dotted line represents GAPDH expression set to 1 (n = 4-6). Protein was quantified using an LC-MS/MS method in males only at ages day 5 and day 60 of PHY treatment (C) (n = 5). Enzyme activity was confirmed by measuring the amount of pentoxyresorufin metabolite produced by S9 fractions isolated from day 5 and day 60 male liver samples (n = 5) treated with resorufin (D). The long-term effects of phenytoin treatment were investigated in a similar fashion. Mice were treated with 100 mg/kg PHY on day 5 of age, then livers were collected (n = 3-6) at different later time points for measurements of mRNA (E), and for protein and enzymatic activity at age day 60 (F and G). The data are presented as mean ± S.E. * $p<0.05$, ** $p<0.01$, and *** $p<0.001$.

Fig. 2. Effects of phenytoin treatment on the expression of CYP2C29 at different ages during postnatal maturation. Male and female mice were treated with either vehicle control (PBS) or 100 mg/kg phenytoin (PHY) at different ages following birth. The short-term effects of PHY treatment were measured 24 hours after treatment. Changes in gene expression were evaluated at

DMD Fast Forward. Published on June 8, 2018 as DOI: 10.1124/dmd.118.080861
This article has not been copyedited and formatted. The final version may differ from this version.

the mRNA level using RT-PCR, then fold-changes were calculated using the $2^{-\Delta\Delta Ct}$ method. Data points represent fold-changes in gene expression of individual mice treated with PBS or PHY compared to average ΔCt of mice that received PBS control (A). Ct values from RT-PCR experiments were also compared to the GAPDH Ct value in each individual mouse and the differences are expressed as $2^{-(Ct(CYP)-Ct(GAPDH))}$ (B). The dotted line represents GAPDH expression set to 1 (n = 4-6). Protein was quantified using an LC-MS/MS method in males only at ages of day 5 and day 60 24 hours after PHY treatment (C) (n = 5). The long-term effects of phenytoin treatment were investigated in a similar fashion. Mice were treated with 100 mg/kg PHY on day 5 of age, then livers were collected (n = 3-6) at different later time points for measurements of mRNA (D) and at day 60 for measurement of protein concentration (E). The data are presented as mean ± S.E. * $p<0.05$, ** $p<0.01$, and *** $p<0.001$.

Fig. 3. Effects of phenytoin treatment on the expression and activity of CYP3A11 at different ages during postnatal maturation. Male and female mice were treated with either vehicle control (PBS) or 100 mg/kg phenytoin (PHY) at different ages following birth. The short-term effects of PHY treatment were measured 24 hours after treatment. Changes in gene expression were evaluated at the mRNA level using RT-PCR, then fold-changes were calculated using the $2^{-\Delta\Delta Ct}$ method. Data points represent fold-changes in gene expression of individual mice treated with PBS or PHY compared to average ΔCt of mice that received PBS control (A). Ct values from RT-PCR experiments were also compared to the GAPDH Ct value in each individual mouse and the differences are expressed as $2^{-(Ct(CYP)-Ct(GAPDH))}$ (B). The dotted line represents GAPDH expression set to 1 (n = 4-6). Protein was quantified using an LC-MS/MS method in males only at ages Day 5 and Day 60 of PHY treatment (C) (n = 5). Enzyme activity was confirmed by measuring the

amount of 1'hydroxymidazolam metabolite produced by S9 fractions isolated from day 5 and day 60 male liver samples (n = 5) treated with midazolam (D). The long-term effects of phenytoin treatment were investigated in a similar fashion. Mice were treated with 100 mg/kg PHY on day 5 of age, then livers were collected (n = 3-6) at different later time points for measurements of mRNA (E), and for protein and enzymatic activity at age of day 60 (F and G). The data are presented as mean ± S.E. * $p<0.05$, ** $p<0.01$, and *** $p<0.001$.

Fig. 4. Effects of phenytoin treatment on the expression of CYP3A16 during postnatal maturation. Male and female mice were treated with either vehicle control (PBS) or 100 mg/kg phenytoin (PHY) at different ages following birth. Twenty-four hours after the treatment, livers were collected for quantification of mRNA by RT-PCR (n = 4-6). Changes in gene expression were evaluated at the mRNA level using RT-PCR, then fold-changes were calculated using the $2^{-\Delta\Delta Ct}$ method. Data points represent fold-changes in gene expression of individual mice treated with PBS or PHY compared to average ΔCt of mice that received PBS control (A). Ct values from RT-PCR experiments were also compared to the GAPDH Ct value in each individual mouse and the differences are expressed as $2^{-(Ct(CYP)-Ct(GAPDH))}$ (B). The dotted line represents GAPDH expression set to 1 (n = 4-6). Protein was quantified using LC-MS/MS 24 hours following phenytoin treatment in male neonates (day 5) and male adults (day 60) (C). The data are presented as mean ± S.E. * $p<0.05$, ** $p<0.01$, and *** $p<0.001$.

DMD Fast Forward. Published on June 8, 2018 as DOI: 10.1124/dmd.118.080861
This article has not been copyedited and formatted. The final version may differ from this version.

Figure 1

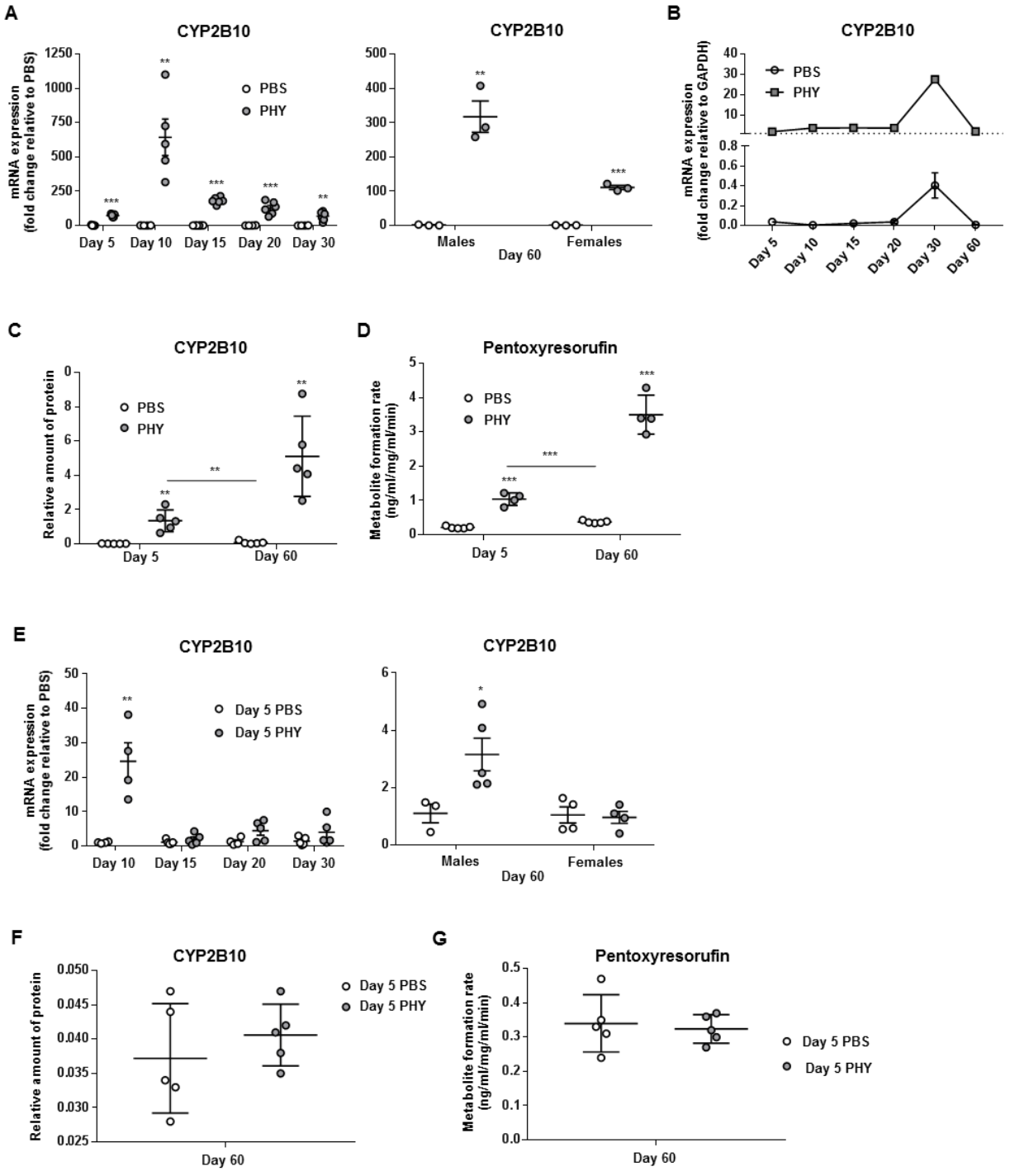

DMD Fast Forward. Published on June 8, 2018 as DOI: 10.1124/dmd.118.080861
This article has not been copyedited and formatted. The final version may differ from this version.

Figure 2

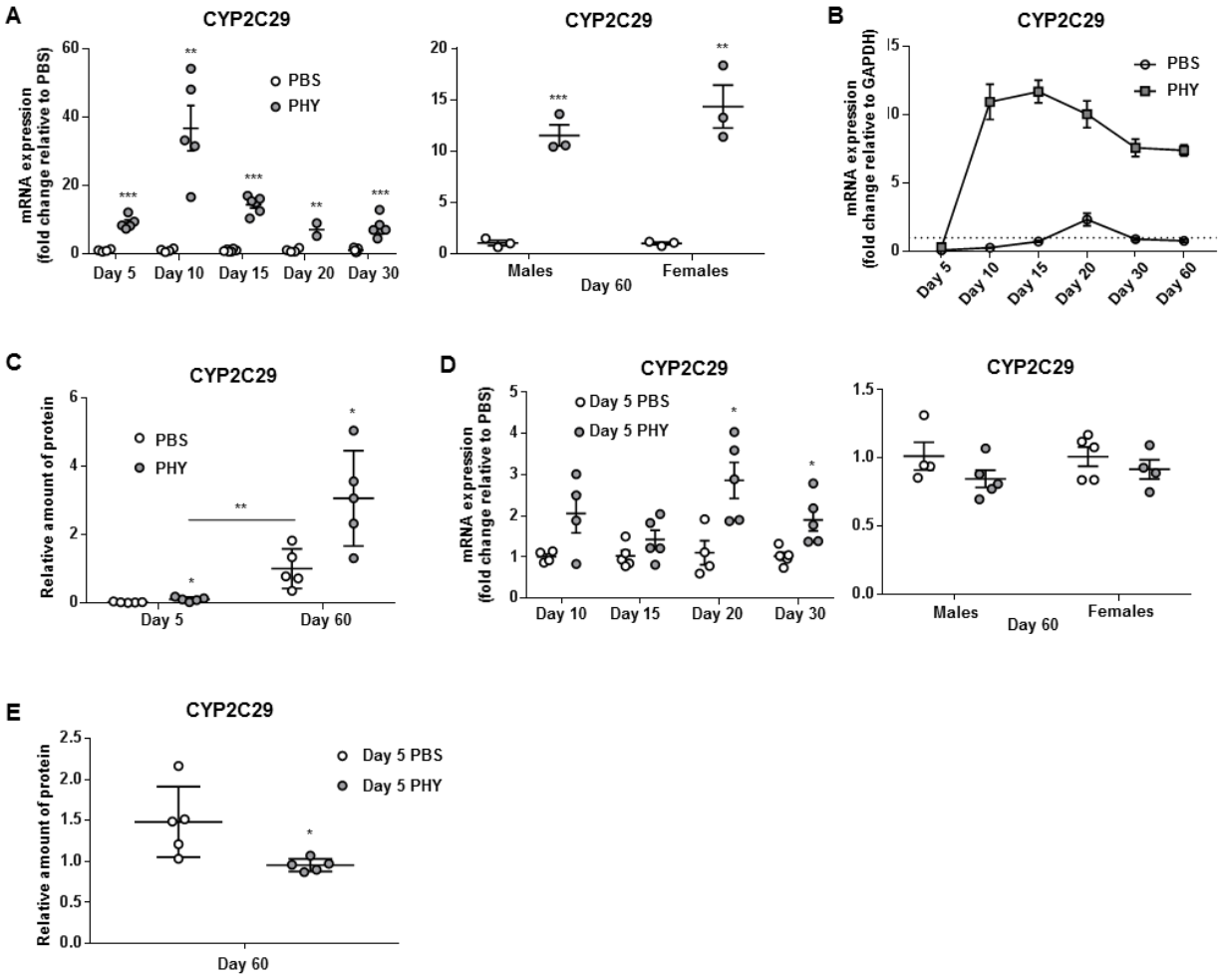

DMD Fast Forward. Published on June 8, 2018 as DOI: 10.1124/dmd.118.080861
This article has not been copyedited and formatted. The final version may differ from this version.

Figure 3

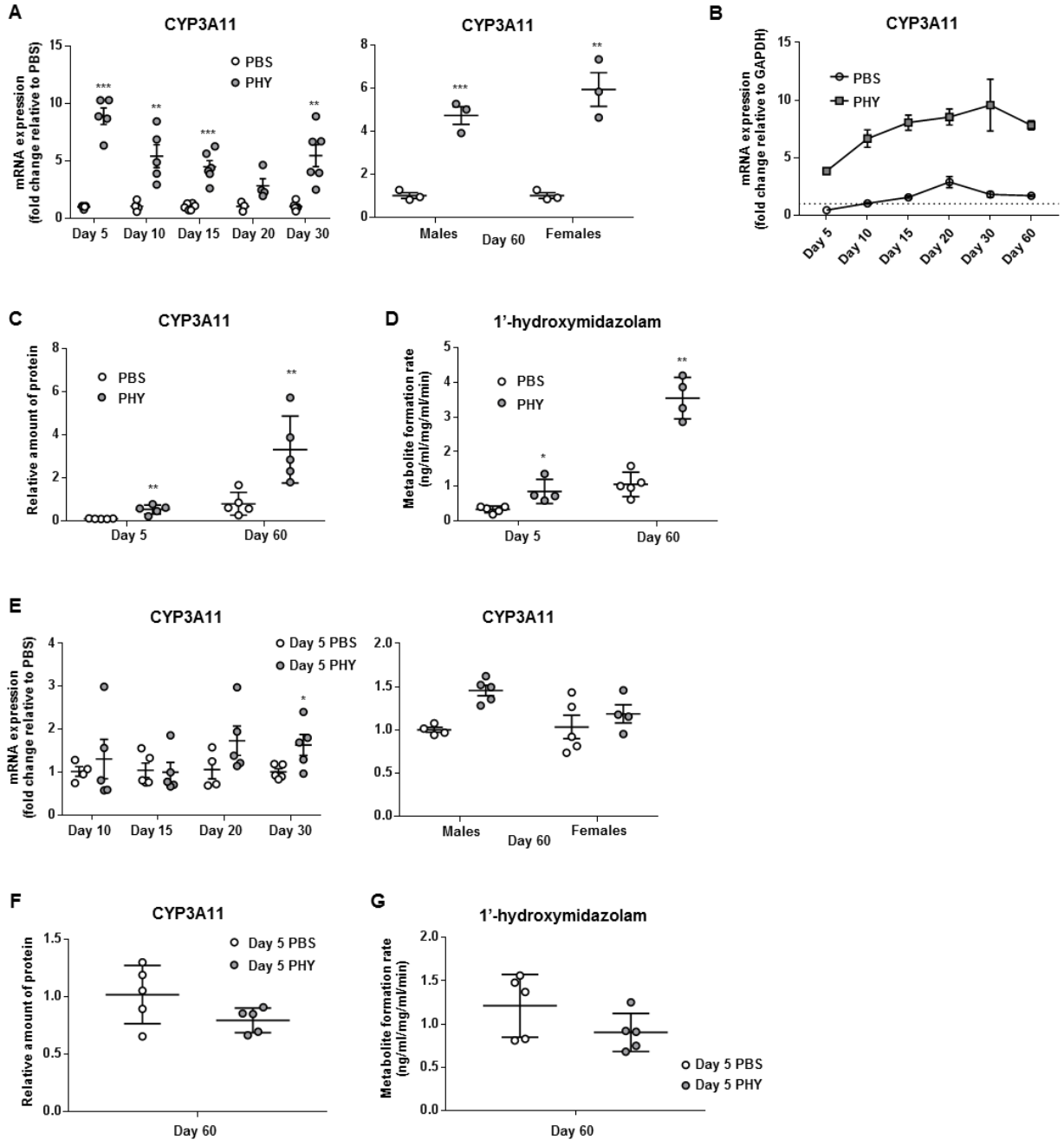

DMD Fast Forward. Published on June 8, 2018 as DOI: 10.1124/dmd.118.080861
This article has not been copyedited and formatted. The final version may differ from this version.

Figure 4